Electronic Supplementary Information

Inherently Chiral Helicene-Substituted Thioalkyl Porphyrazine Complexes: Synthesis, Electronic, and Chiroptical Properties

Sandra Belviso*[a], Giulia Marsico[a], Roberta Franzini[b], Claudio Villani[b], Sergio Abbate[c,d], Giovanna Longhi*[c,d]

[a]Dipartimento di Scienze, Università della Basilicata, Viale dell'Ateneo Lucano 10, 85100 Potenza, Italy

[b]Dipartimento di Medicina Molecolare e Traslazionale, Università di Brescia, Viale Europa 11, 25123 Brescia, Italy

[c]Dipartimento di Chimica e Tecnologie del Farmaco, Università di Roma "La Sapienza", Piazzale Aldo Moro 5, 00185 Roma, Italy

[d]I.N.O.-CNR Unit of Brescia, c/o CSMT via Branze, 45 – 25123 Brescia, Italy

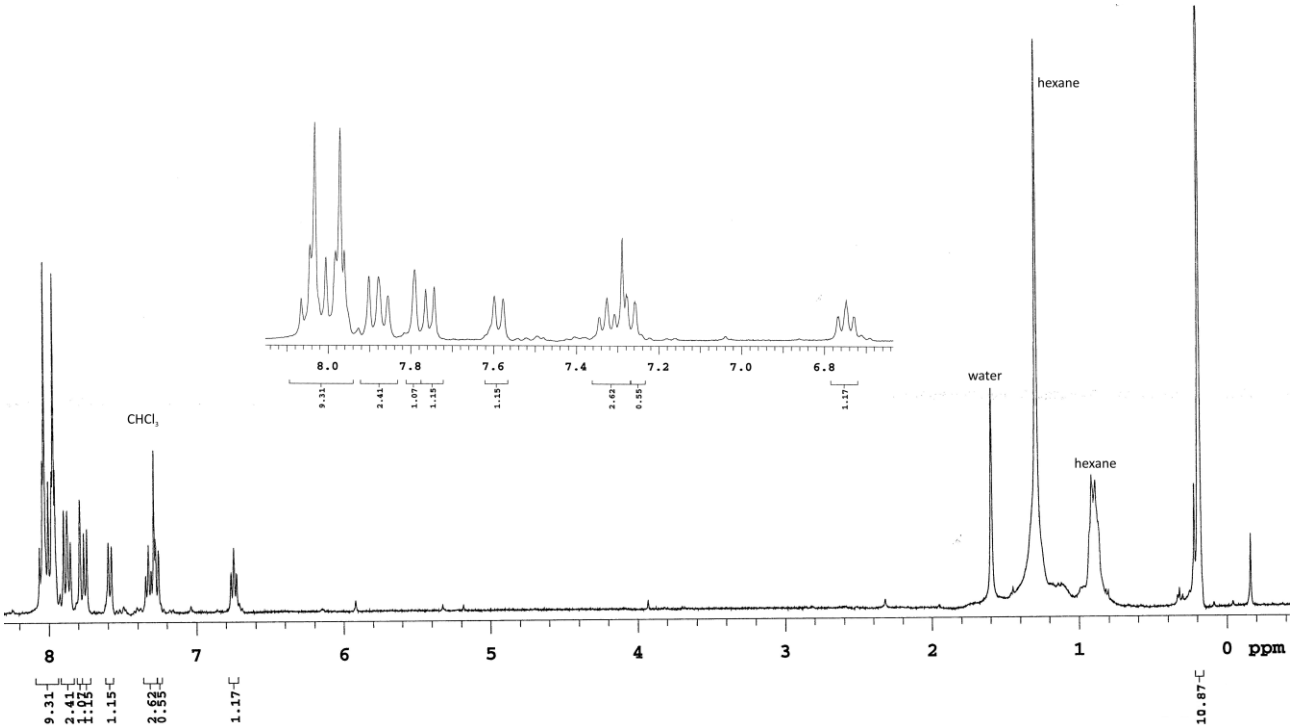

Figure S1. ^{1}HNMR spectrum of compound **2** in $CDCl_3$.

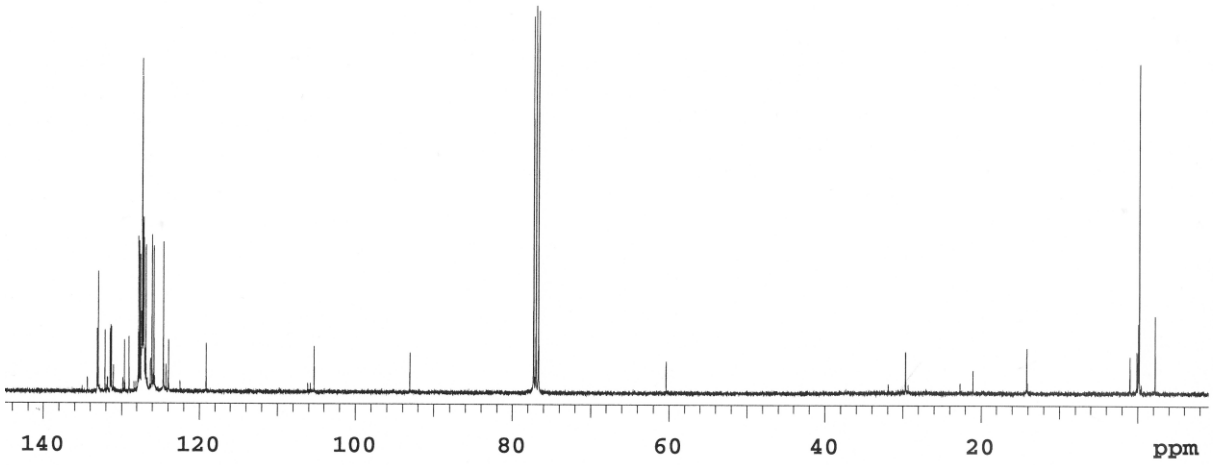

Figure S2. ^{13}CNMR spectrum of compound **2** in $CDCl_3$.

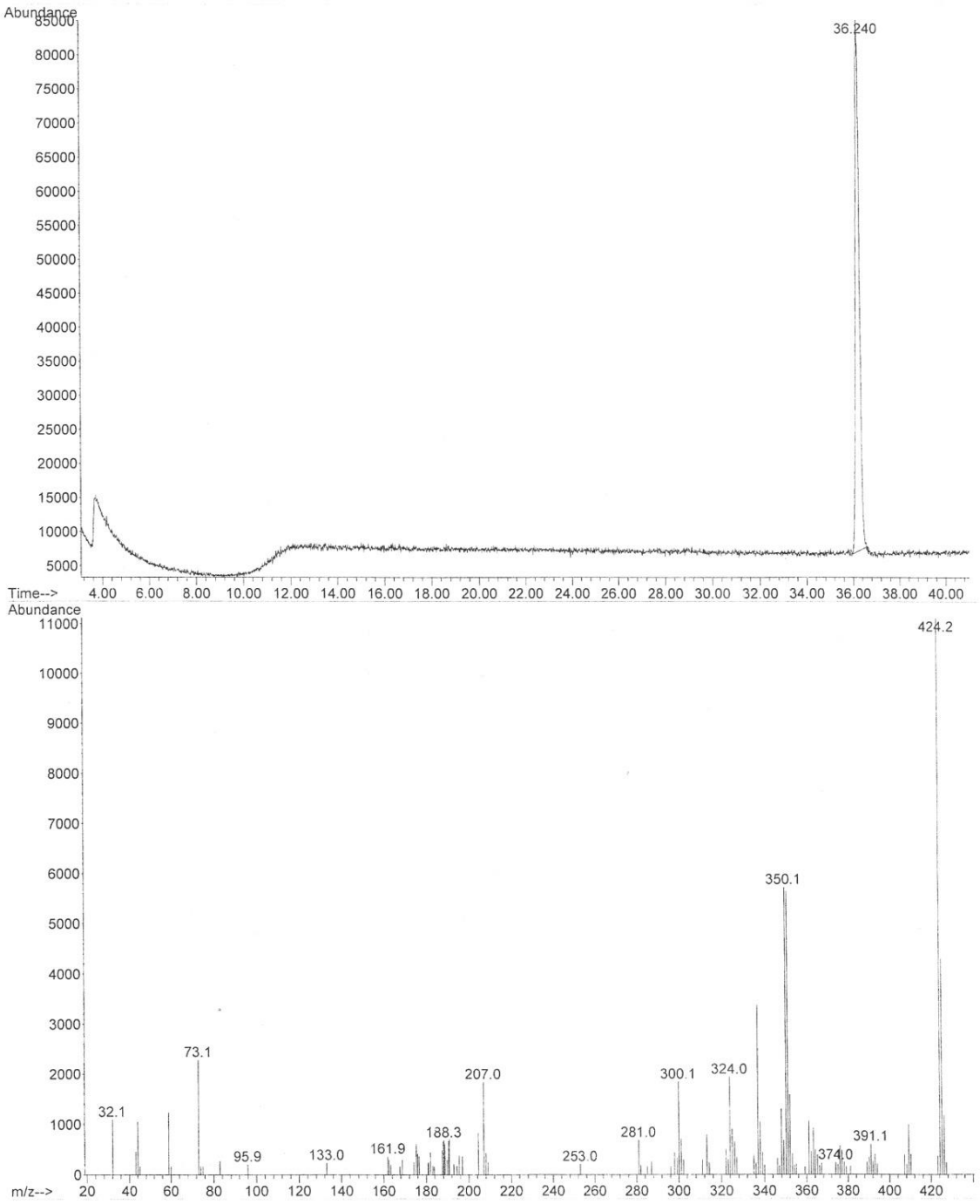

Figure S3. GC-MS spectrum of compound **2** in $CDCl_3$.

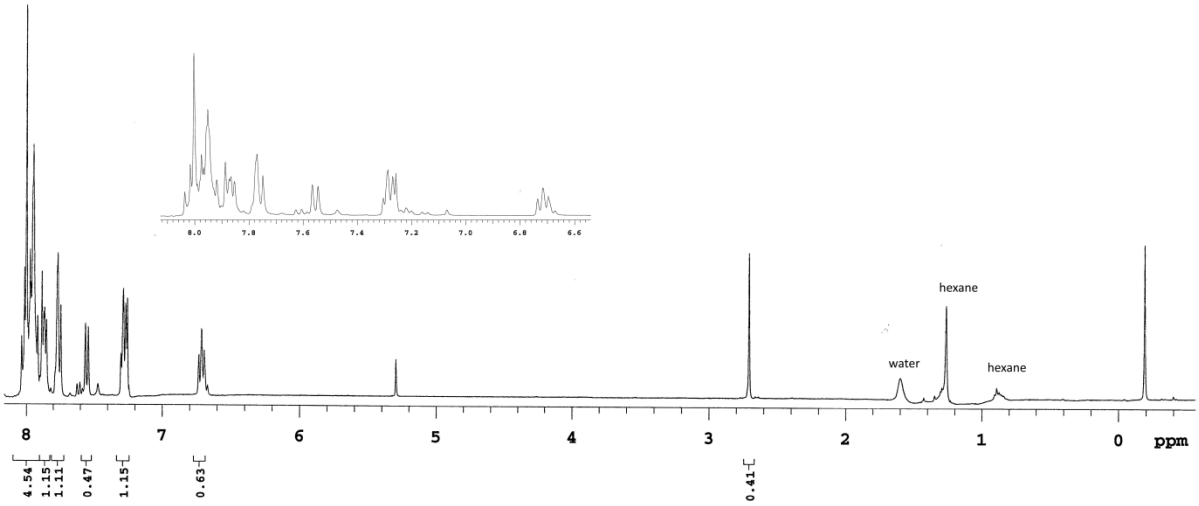

Figure S4. ^{1}HNMR spectrum of compound **3** in $CDCl_3$.

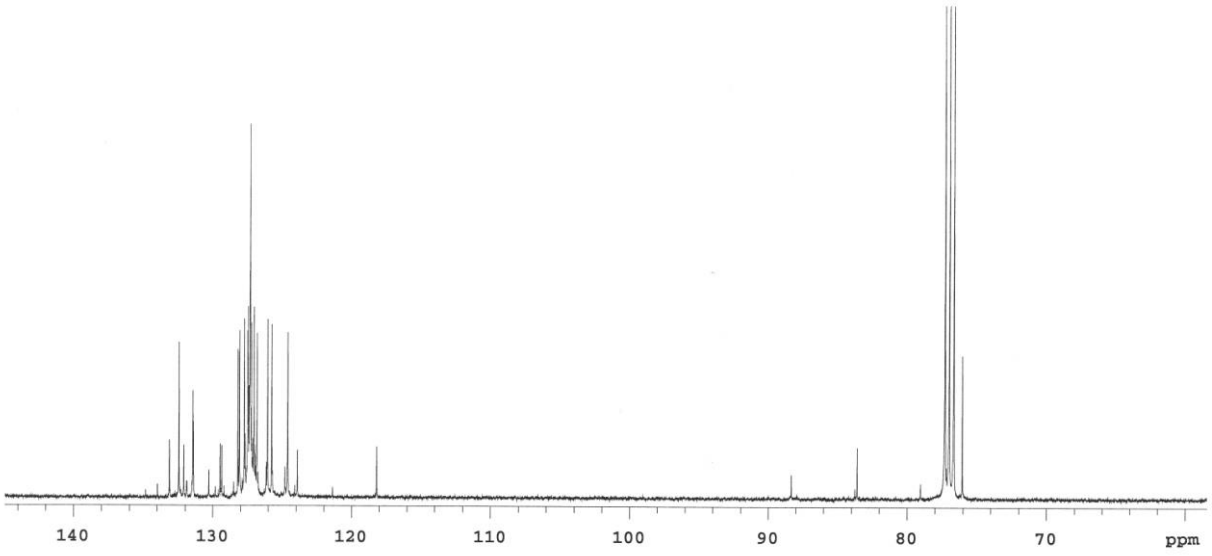

Figure S5. ^{13}CNMR spectrum of compound **3** in $CDCl_3$.

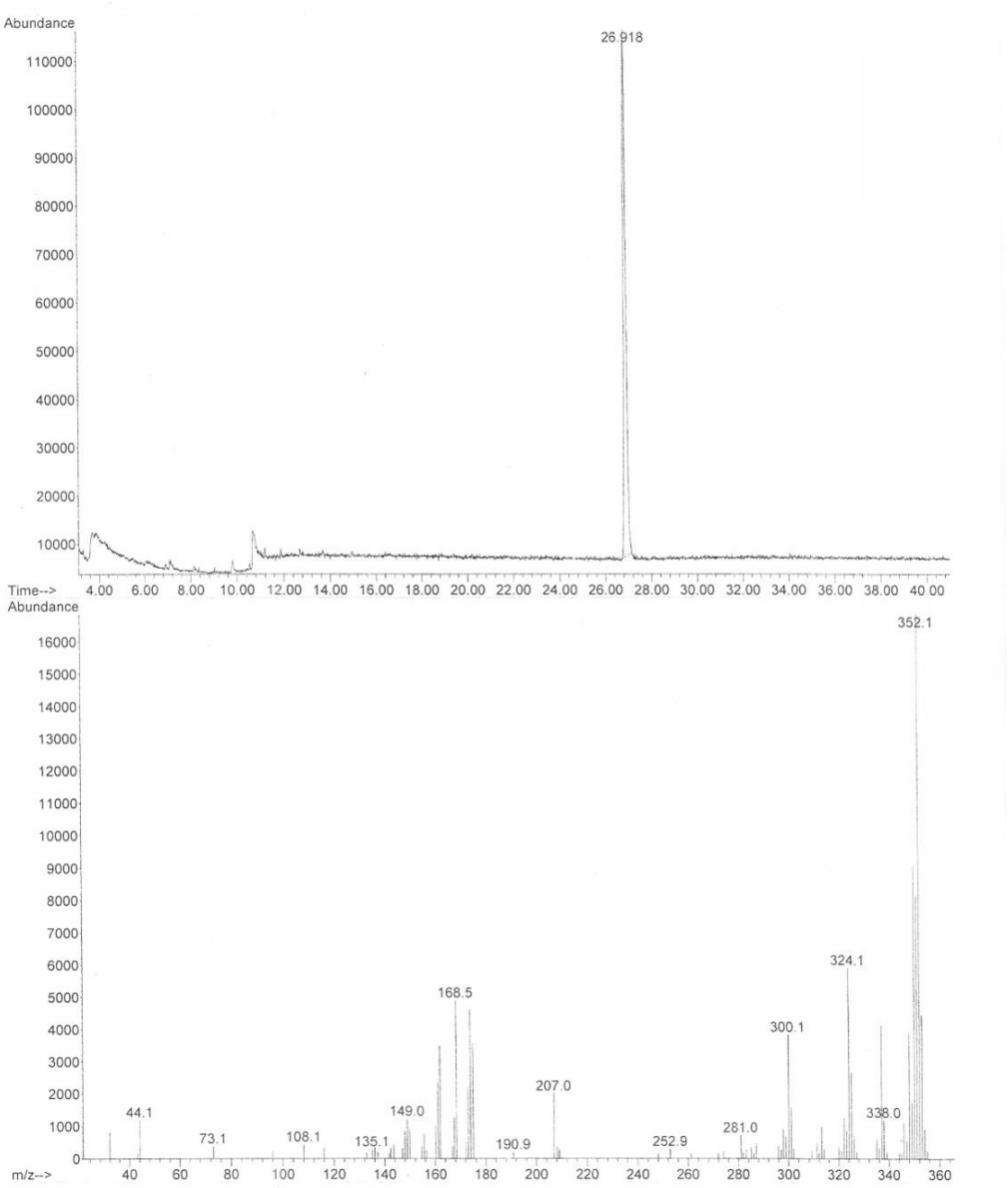

Figure S6. GC-MS spectrum of compound **3** in $CDCl_3$.

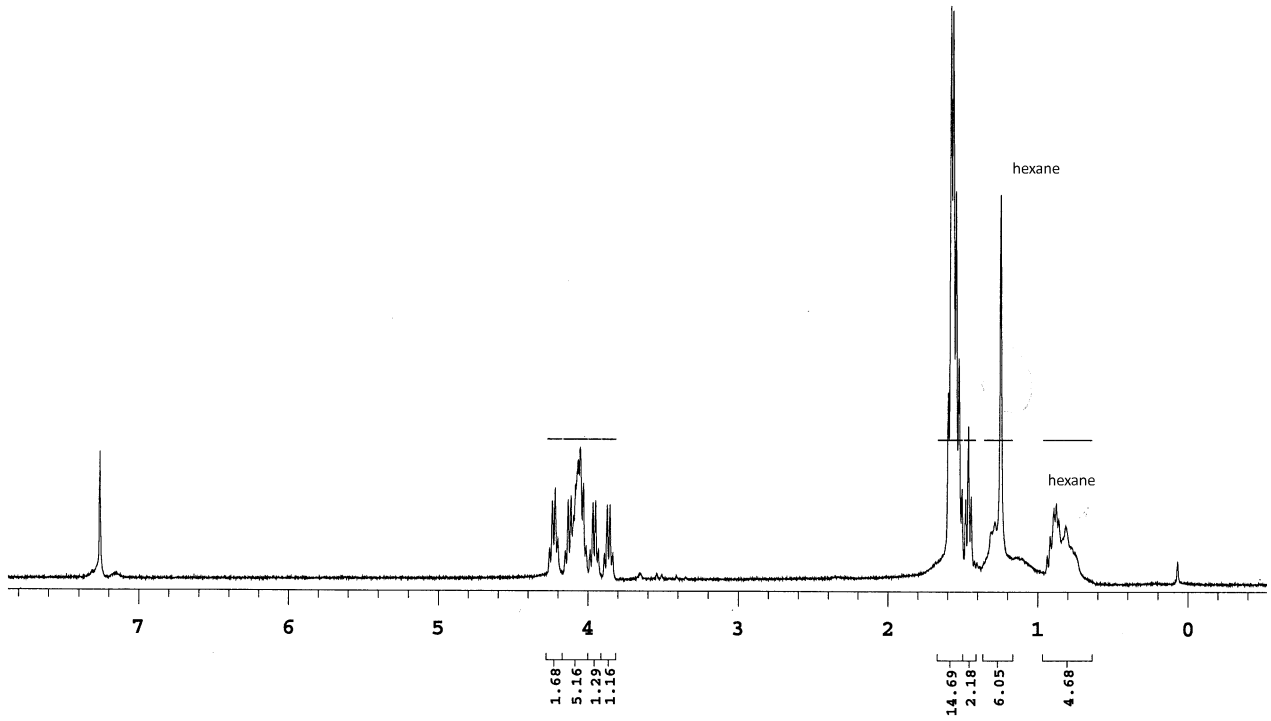

Figure S7. ^{1}HNMR spectrum of compound **6c** in $CDCl_3$.

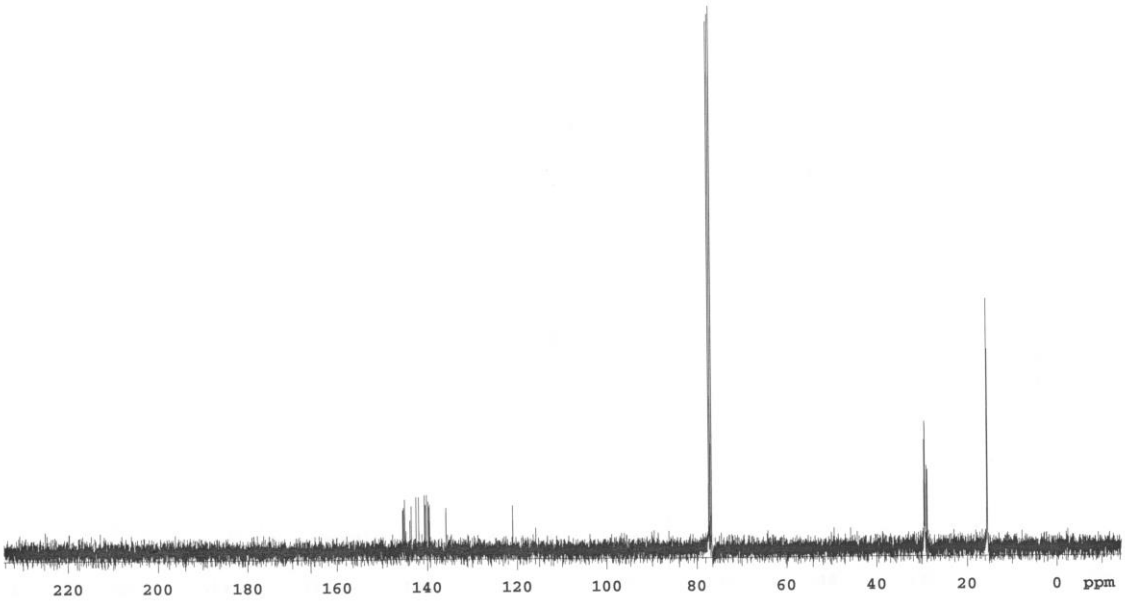

Figure S8. ^{13}CNMR spectrum of compound **6c** in $CDCl_3$.

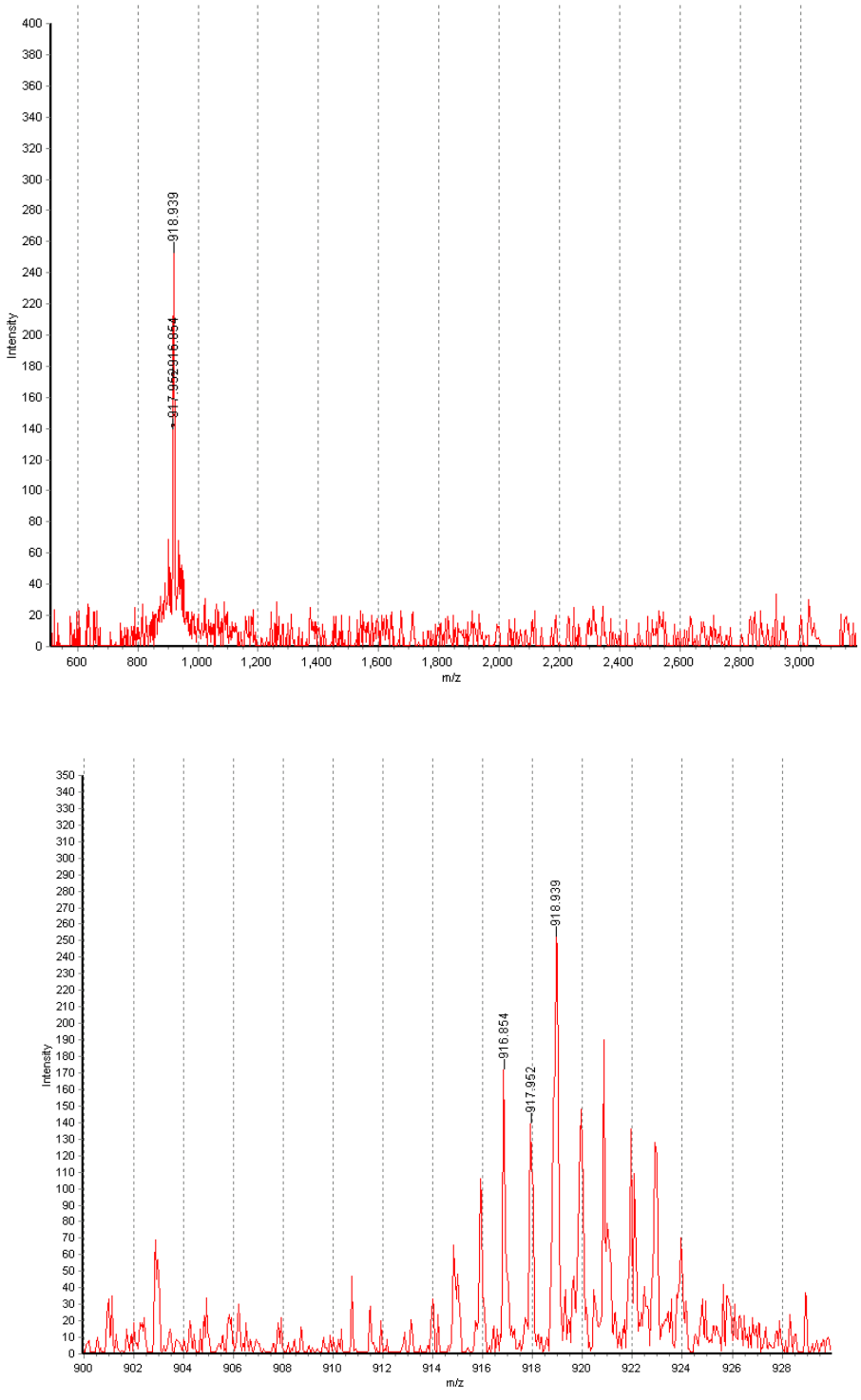

Figure S9. MALDI-TOF MS spectrum of **6c**.

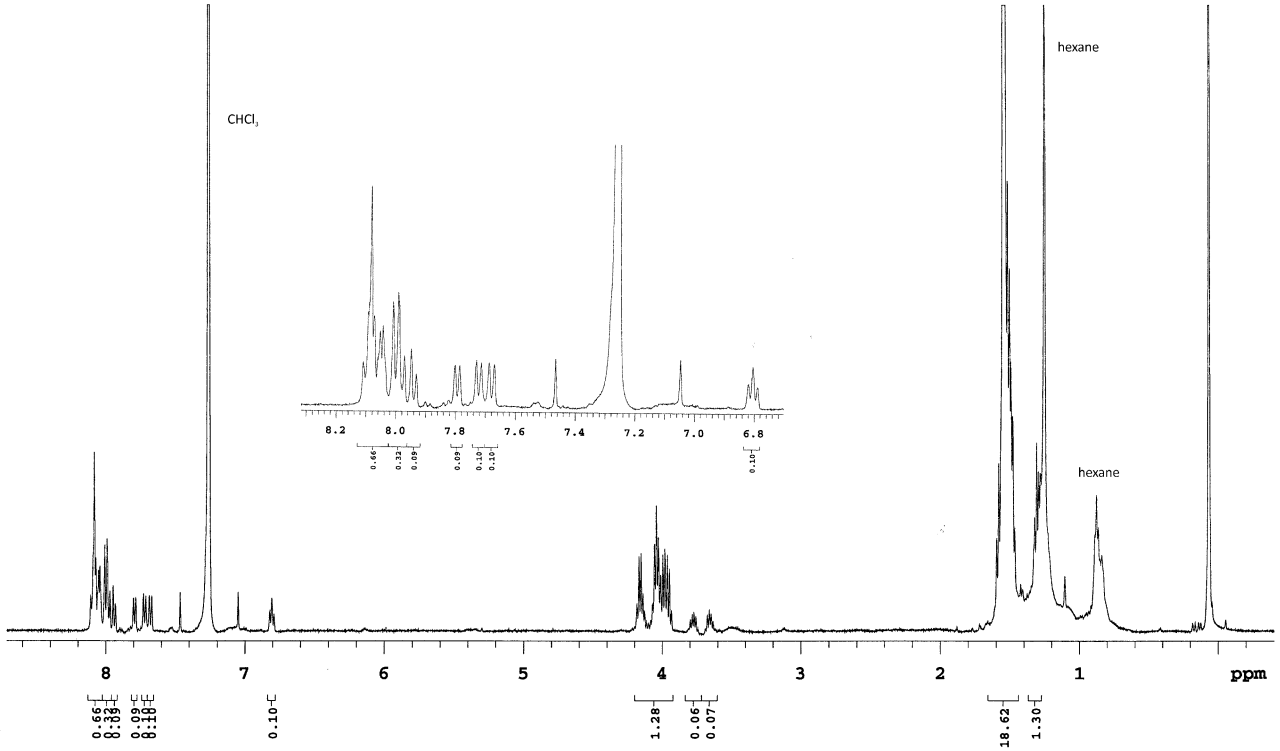

Figure S10. ^{1}HNMR spectrum of compound **NiPzHelix** in $CDCl_3$.

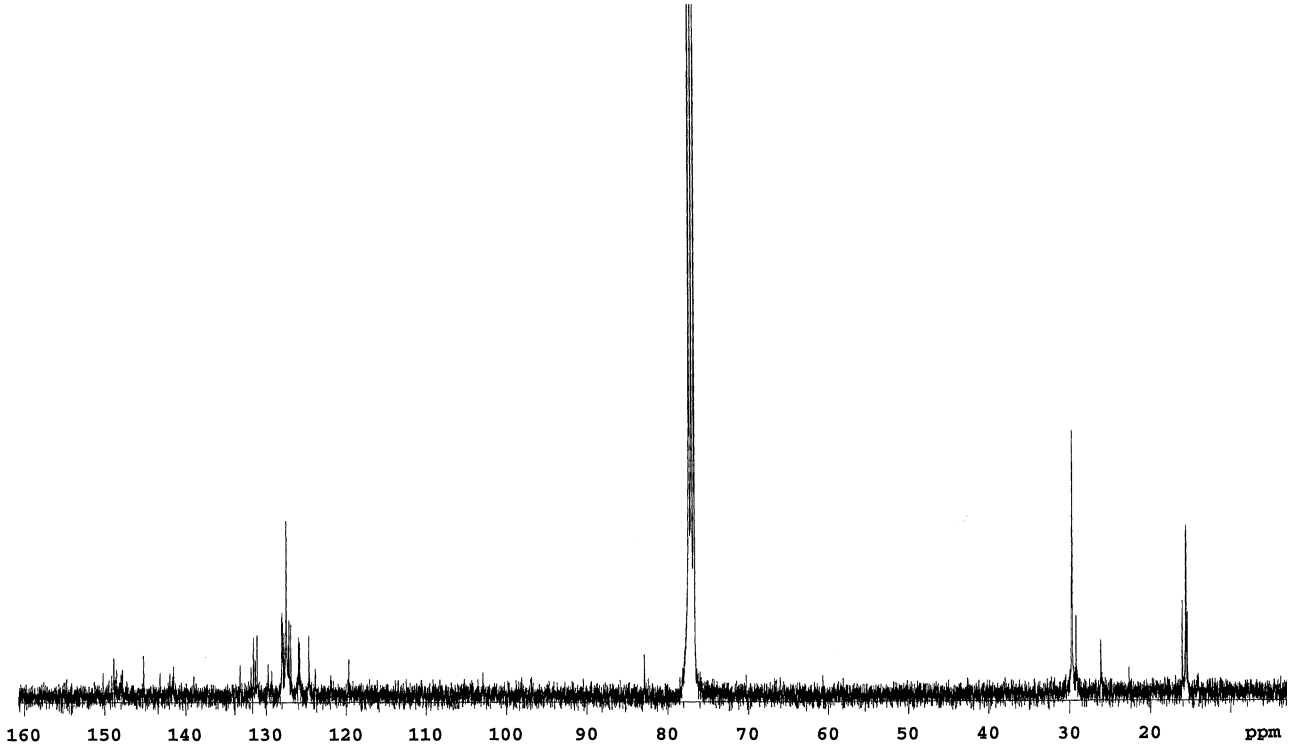

Figure S11. ^{13}CNMR spectrum of compound **NiPzHelix** in $CDCl_3$.

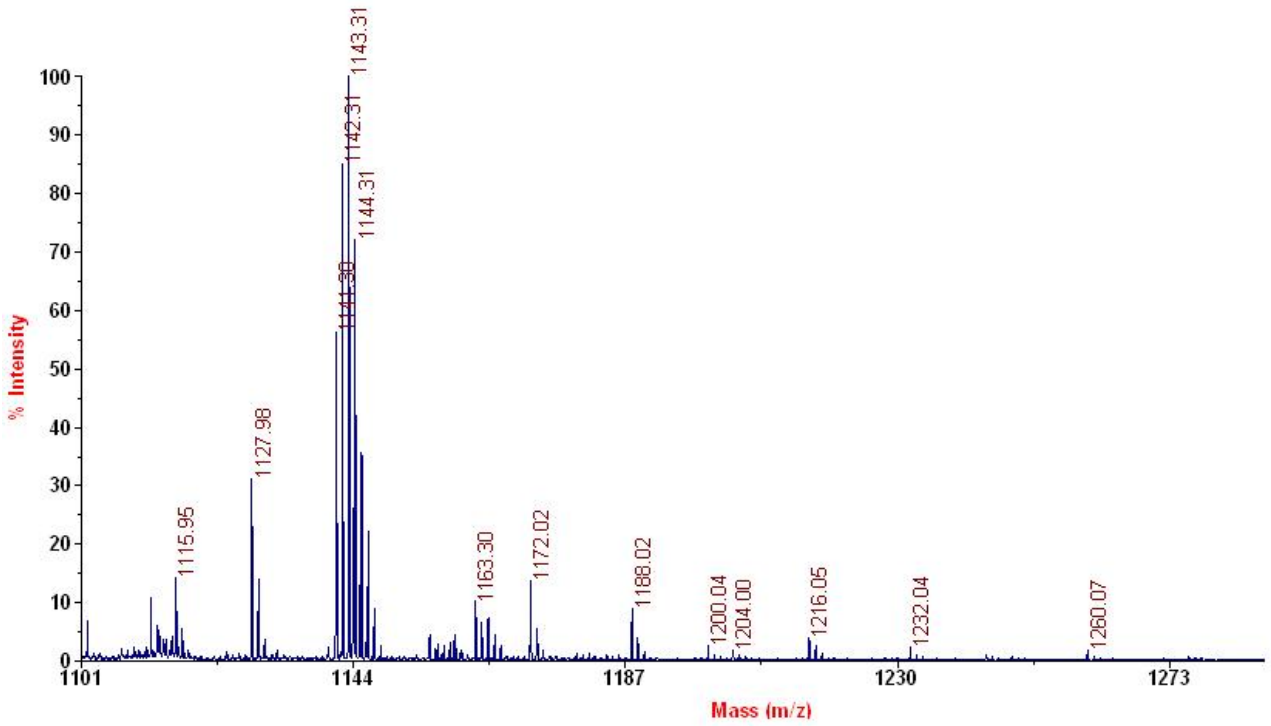

Figure S12. MALDI-TOF MS spectrum of **NiPzHelix**.

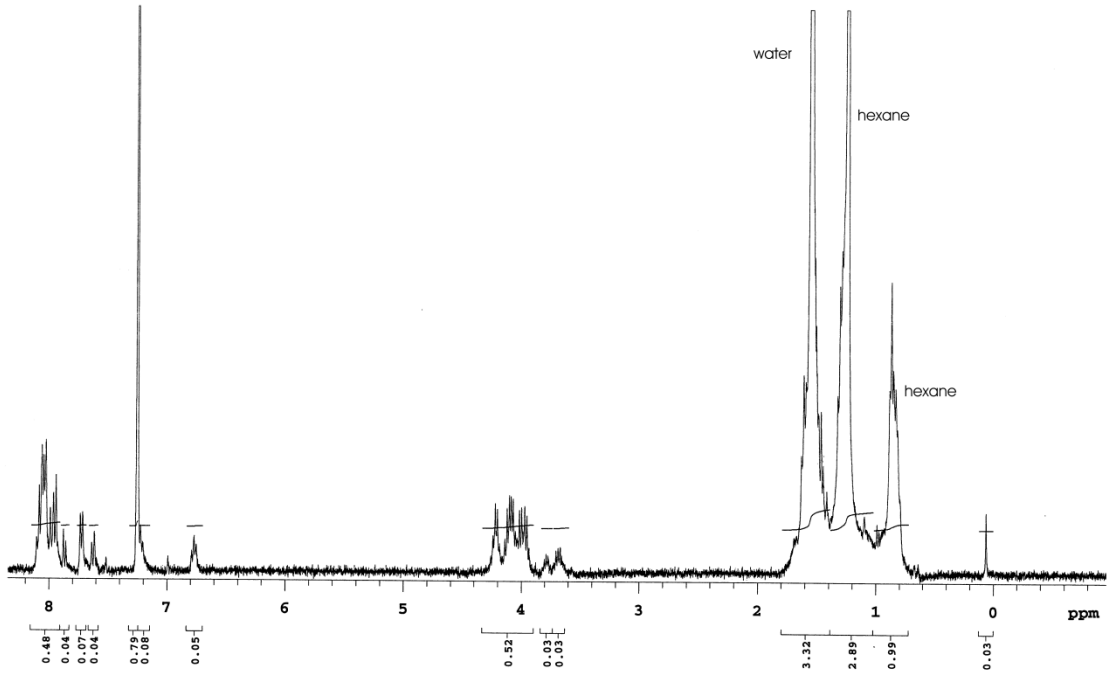

Figure S13. ^{1}HNMR spectrum of compound **PdPzHelix** in $CDCl_3$.

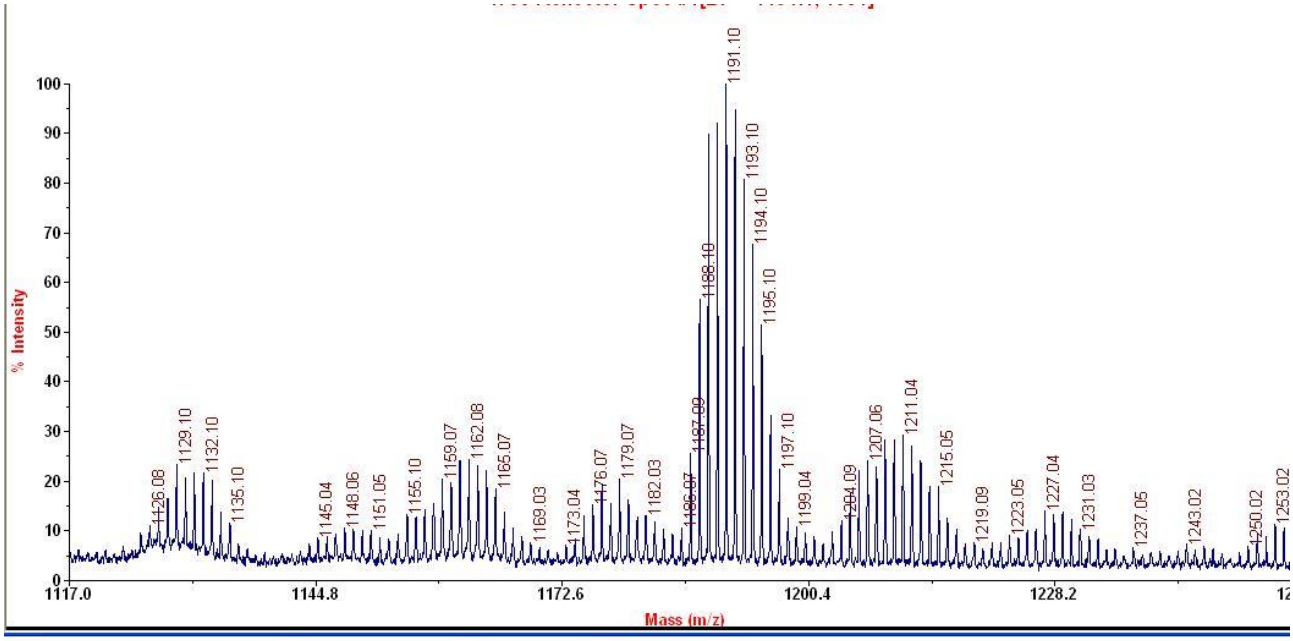

Figure S14. MALDI-TOF MS spectrum of **PdPzHelix**.

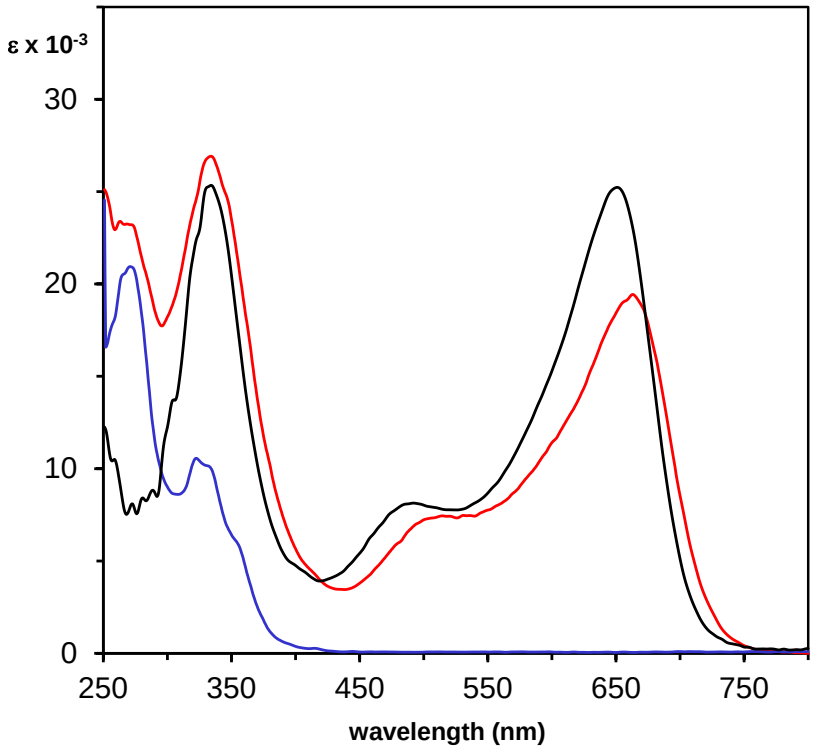

Figure S15. UV-vis spectra (CH_2Cl_2) of 2-ethynyl hexahelicene (**3**) (blue line), Pd(II) complex **6c** (black line), and **PdPzHelix** (red line).

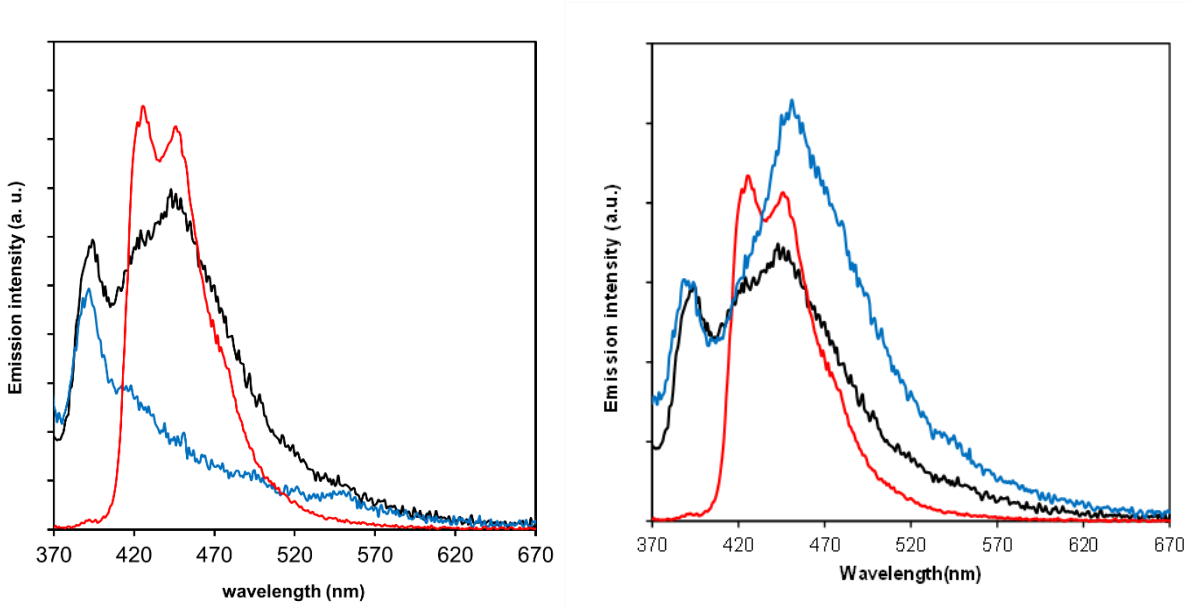

Figure S16. (a) Left: Comparison of the emission spectrum (CH_2Cl_2, λ_{exc} 350 nm) of **NiPzHelix** (*c* = 8.4×10^{-6} M black line), of 2-ethynyl hexahelicene (**3**) (*c* = 1.4×10^{-6} M, red line) and of Ni(II) complex **Ni-4** (c = 1.0×10^{-5} M, blue line). (b) Right: comparison of the emission spectrum (CH_2Cl_2, λ_{exc} 350 nm) of **NiPzHelix** (*c* = 8.4×10^{-6} M black line), of **PdPzHelix** (*c* = 9.2×10^{-6} M blue line), of 2-ethynyl hexahelicene (**3**) (*c* = 1.4×10^{-6} M, red line).

DFT Calculations.

Calculations have been conducted on a model compound with SCH_3 pendant groups to avoid too many conformers. The helicene P enantiomer has been considered.

Considering the *up* (*u*) and *down* (*d*) orientation of the pendant groups, notation already introduced in references [1] and [2], the thioalkyl chains of **Ni-4** manifest the lowest energy conformation with the up-up-down-down orientation (*uudd*). In **NiPzHelix** case the presence of a bulky substituent influences the conformation of the nearby groups. A conformational search permits to identify the most stable conformers

Table S1. **NiPzHelix**: Geometrical and energy characteristics of the principal optimized conformers. Optimization at bp86/ 6-31+G* level, LANL2DZ pseudopotential for Ni.

	Kcal/mol	**pop**	τ1	τ2	τ3	τ4	τ5	τ6	τ7	Approx.
a	0.00	*54.5%*	140	-134	-136	138	128	-174	11	*dduud00*
b	0.48	*24.3%*	144	-133	-138	135	137	-134	-140	*dduuddu*
c	0.56	*21.2%*	169	-126	-138	137	127	-172	-8	*0duud00*
d	1.75	*2.8%*	143	135	129	-162	-26	128	137	*dud00ud*
e	2.21	*1.3%*	144	132	137	133	136	133	137	*dududud*

Definition of reported dihedral angles: τ1 (red), τ2 (green) and analogously for all subsequent CCSC torsions.

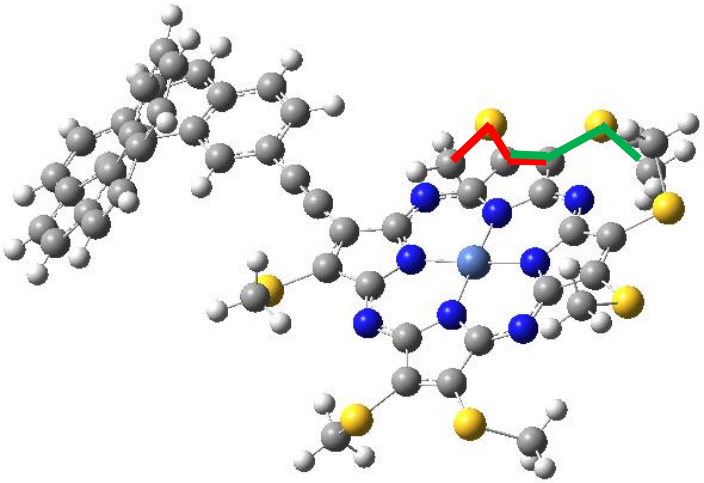

[1] A. Rosa, G. Ricciardi, E. J. Baerends, M. Zimin, M. A. J. Rodgers, S. Matsumoto, N. Ono, *Inorg. Chem*. **2005**, *44*, 6609−6622.

[2] S. Ghidinelli, S. Abbate, E. Santoro, S. Belviso, G. Longhi, *J. Phys. Chem. B* **2021**, *125*, 264–280.

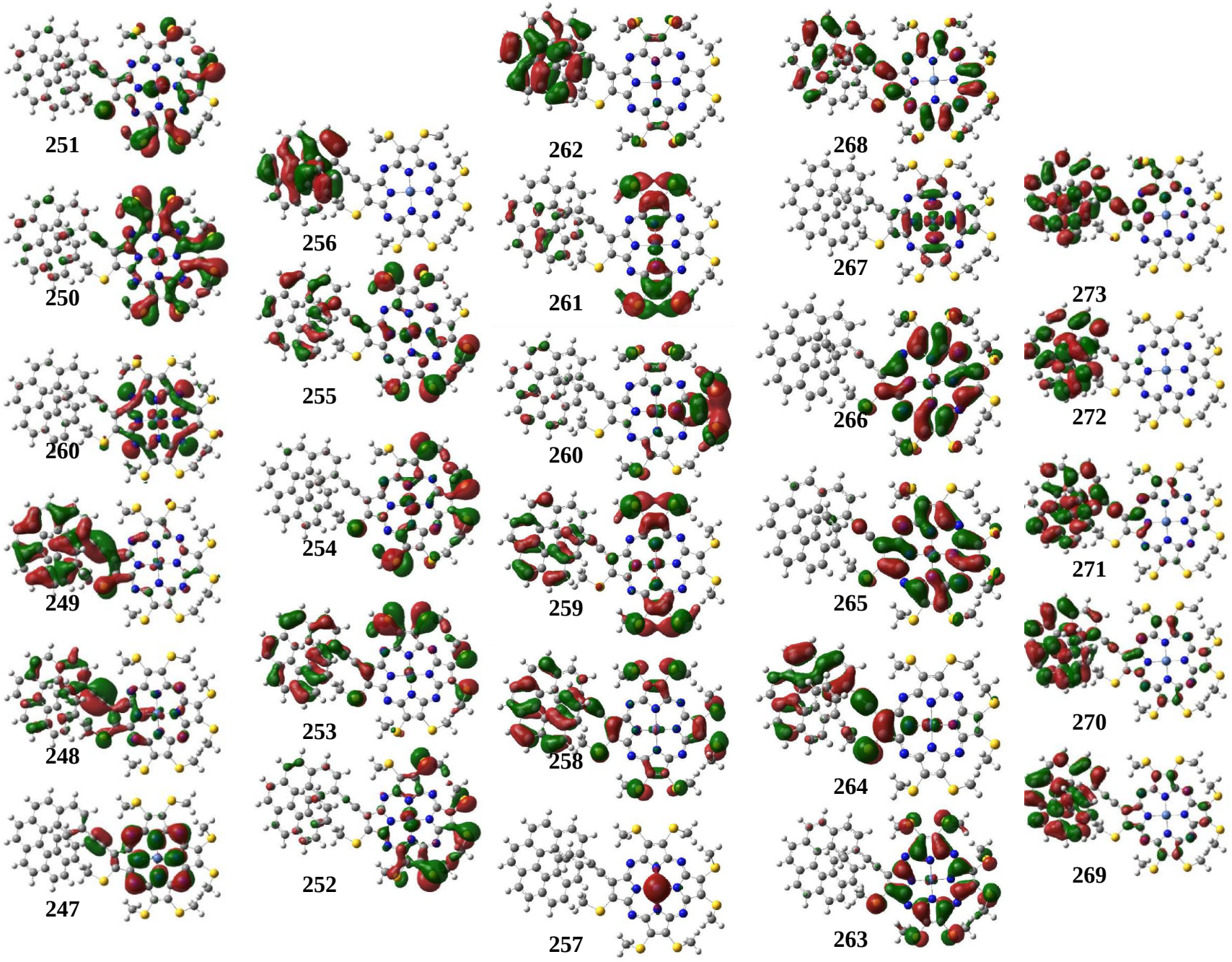

Figure S17. Kohn–Sham orbital graphical representations of some more relevant orbitals used to describe the transitions in Table S2 for **NiPzHelix**.

Table S2. NiPzHelix: Spectroscopic characteristics of the main calculated transitions: wavelength λ (nm), oscillator strength f, rotational strength R (esu^2cm^2), KS energy levels. Color code refer to the type of orbital: red, Gouterman orbital; yellow, orbital localized on Pz; green, orbital with major contribution from nickel; blue, orbital mainly localized on helicene; light blue, orbital localized on helicene and triple bond bridge; purple, orbital on the bridge; black, delocalized orbital.

#	λ	f	R																
1	912	0.024	-1.8	264	heli-b	265	Gout.	-0.48	264	heli-b	266	Gout.	0.51						
2	875	0.091	-9.2	264	heli-b	265	Gout.	0.51	264	heli-b	266	Gout.	0.48						
7	741	0.008	13.4	261	Pz	266	Gout.	0.59	261	Pz	265	Gout.	-0.21	262	helicene	266	Gout.	-0.20	
9	722	0.059	16.0	260	Pz	266	Gout.	0.50	263	Gout.	265	Gout.	-0.27	263	Gout.	266	Gout.	-0.24	
10	714	0.052	-30.2	259	deloc.	265	Gout.	0.39	263	Gout.	265	Gout.	0.35	260	Pz	265	Gout.	0.31	
11	693	0.078	26.5	259	deloc.	266	Gout.	0.45	263	Gout.	266	Gout.	0.36	258	deloc.	266	Gout.	-0.22	
17	649	0.052	-70.6	257	Ni	265	Gout.	0.51	258	deloc.	266	Gout.	-0.30	257	Ni	266	Gout.	-0.23	
18	644	0.163	126.8	257	Ni	266	Gout.	0.45	259	deloc.	266	Gout.	0.29	258	deloc.	265	Gout.	-0.27	
19	637	0.085	-65.1	257	Ni	266	Gout.	0.41	258	deloc.	266	Gout.	-0.35	260	Pz	267	Ni	0.28	
20	624	0.215	20.8	261	Pz	267	Ni	0.48	258	deloc.	266	Gout.	-0.25	263	Gout.	266	Gout.	-0.21	
21	615	0.121	-33.9	260	Pz	267	Ni	0.61	257	Ni	266	Gout.	-0.20						
34	490	0.145	63.1	264	heli-b	268	deloc.	0.53	252	Pz	266	Gout.	-0.32	251	Pz	265	Gout.	0.19	
35	489	0.105	174.0	252	Pz	266	Gout.	0.44	264	heli-b	268	deloc.	0.36	252	Pz	265	Gout.	-0.34	
71	391	0.029	172.0	260	Pz	270	heli	0.48	262	heli	269	heli	-0.22	258	deloc.	269	heli	0.22	
72	381	0.042	221.9	256	heli	268	deloc.	0.47	264	heli-b	271	heli	0.30	258	deloc.	269	heli	0.27	
76	373	0.062	163.9	256	heli	268	deloc.	0.39	258	deloc.	270	heli	0.32	264	heli-b	271	heli	-0.27	
77	371	0.108	-110.6	255	deloc.	268	deloc.	0.49	245	->	265	Gout.	-0.24	264	heli-b	271	heli	-0.23	
81	364	0.138	-16.6	254	Pz	268	deloc.	0.64	246	Gout.	265	Gout.	-0.14						
90	354	0.455	-47.6	246	Gout.	265	Gout.	0.25	247	bridge	267	Ni	-0.23	264	heli-b	272	heli	0.21	
				246	Gout.	267	Ni	-0.21	261	Pz	271	heli	0.21	253	deloc.	268	deloc.	-0.19	
93	351	0.112	-6.4	246	Gout.	267	Ni	0.47	261	Pz	271	heli	-0.33	260	Pz	271	heli	0.11	
94	350	0.152	5.4	256	heli	269	heli	0.34	246	Gout.	266	Gout.	-0.26	246	Gout.	265	Gout.	-0.23	
95	349	0.136	-99.7	256	heli	269	heli	0.41	255	deloc.	269	heli	-0.26	242	->	265	Gout.	0.22	
101	343	0.112	-53.5	260	Pz	271	heli	0.43	242	->	266	Gout.	-0.33	254	Pz	269	heli	0.19	
145	303	0.146	-121.8	264	heli-b	273	heli	0.25	249	Pz	269	heli	0.24	258	deloc.	272	heli	0.23	

Absorption and ECD spectrum of **NiPzHelix** has been calculated at the M06-L/6-31+G* level, LANL2DZ pseudopotential for Ni on the previously optimized geometry considering solvent with iefpcm model.

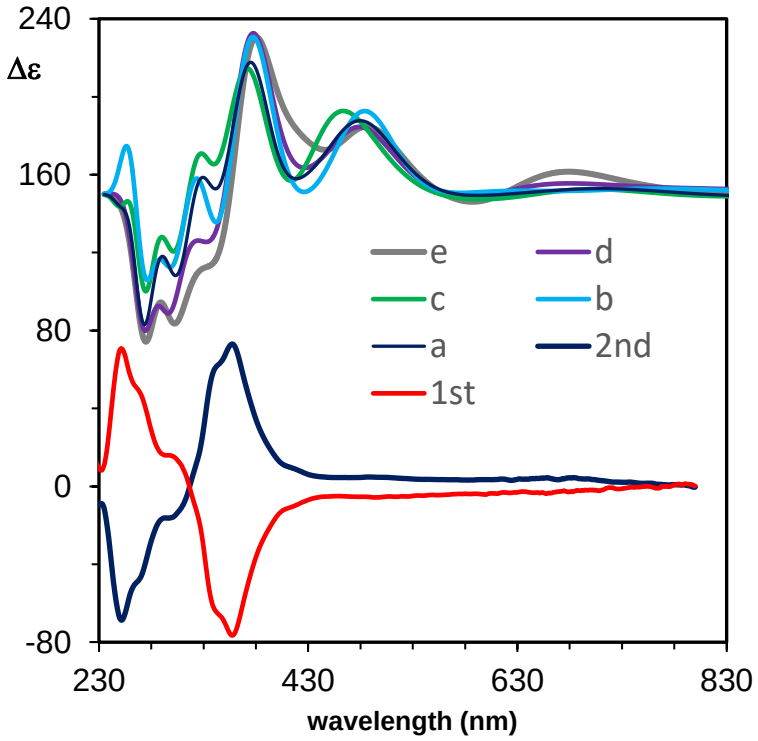

Figure S18. Calculated ECD spectra for the five principal conformers of **NiPzHelix**.

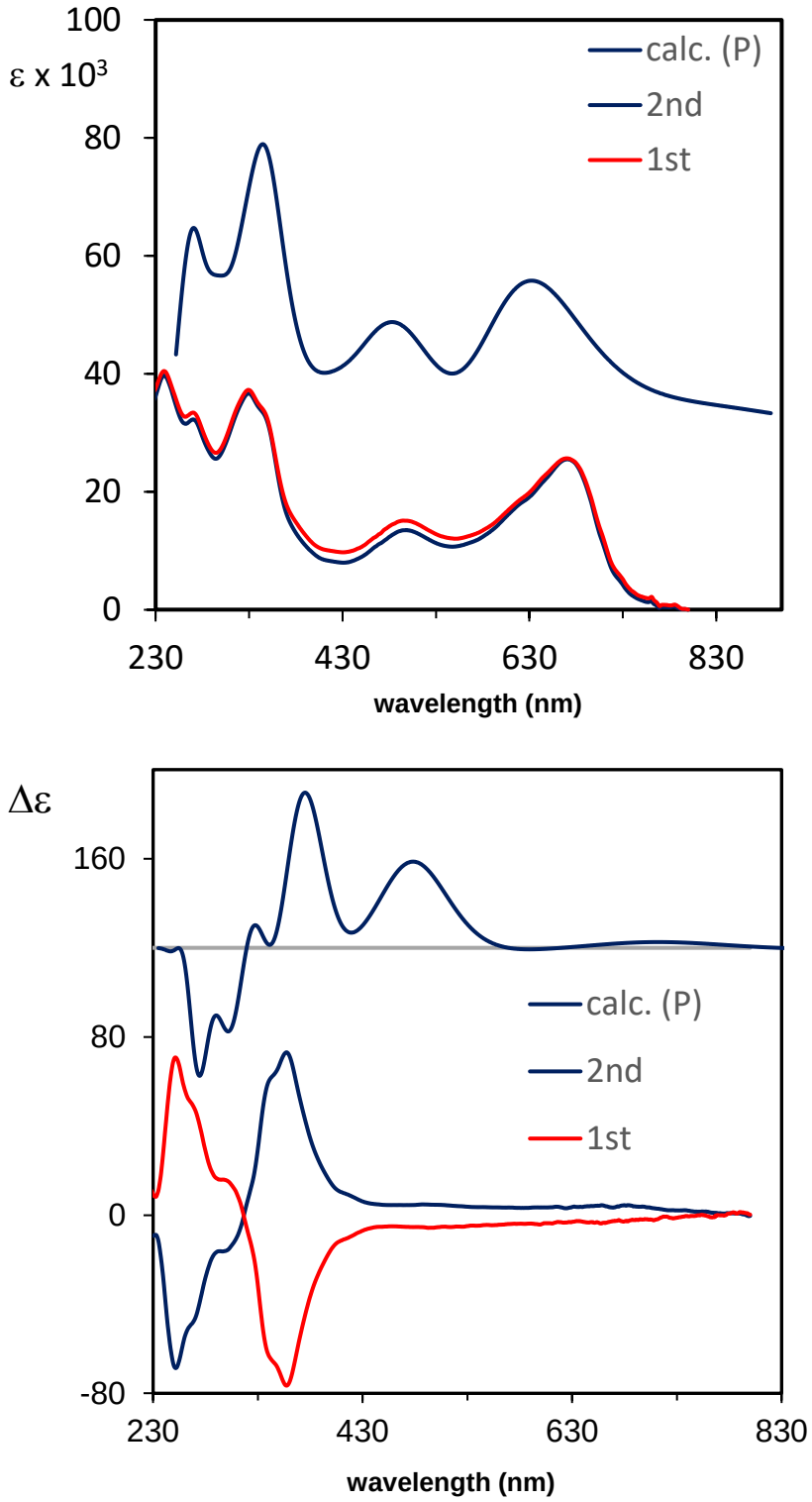

Figure S19. Calculated absorption and ECD spectra of **NiPzHelix**, after average over the five principal conformers in comparison with the experimental spectra obtained on the two eluted fractions. (bp86/6-31+G*//m06l//6-31+G*; iefpcm CH_2Cl_2).

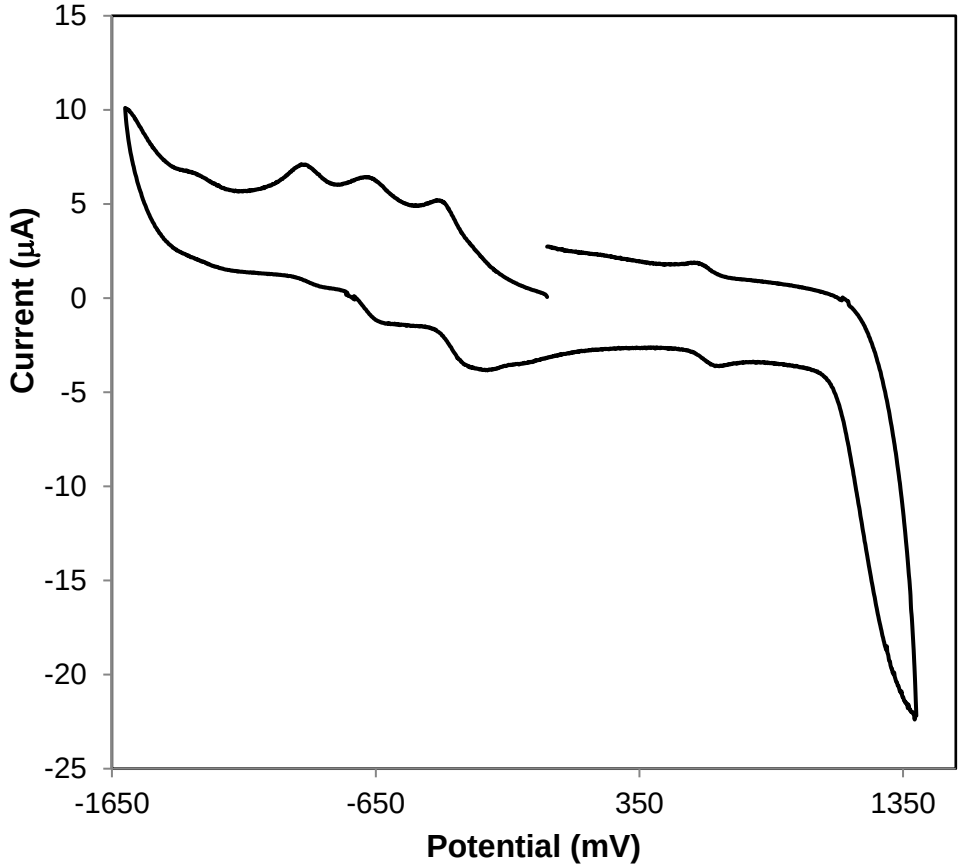

Figure S20. Cyclic voltammogram of **PdPzHelix** complex in CH_2Cl_2.